AUTONOMOUS NAVIGATION FOR ORCHARD INTER-TREE WEEDING ROBOTS BASED ON AN IMPROVED A*-DWA FUSION ALGORITHM
/
基于改进 A*-DWA 融合算法的果园株间除草机器人自主导航研究

Yan XU, Qing YUAN, Dazhong WANG, Yinan LIU, Xiangchen MENG, Xiang YUE
College of Engineering, Shenyang Agricultural University, Shenyang, China
Corresponding author: Xiang Yue
Tel: +8613940305658.; E-mail: yuexiang@syau.edu.cn
DOI: https://doi.org/10.35633/inmateh-79-88

Keywords: *Orchard inter-tree weeding robots; Autonomous navigation; A*-DWA fusion algorithm; Path planning; Obstacle avoidance*

ABSTRACT
Aiming at autonomous weeding in narrow, complex orchards, this paper proposes an improved A and DWA fusion path planning algorithm. Globally, a safety distance penalty in the A* cost function prevents paths from adhering to tree trunks. Locally, enhanced DWA modules, including dynamic obstacle angle thresholds, hierarchical lateral braking, and adaptive velocity window expansion, resolve trajectory oscillation and local minima. Validated in real orchards, the algorithm achieved a 0.029 m tracking deviation and over 95% dynamic obstacle avoidance success rate, providing robust and safe navigation for autonomous robots.*

摘要
针对狭窄、复杂的果园自主除草场景，本文提出了一种改进的 A 与 DWA 融合路径规划算法。在全局规划中，A 代价函数中的安全距离惩罚项可防止路径过分紧贴树干。在局部规划中，增强的 DWA 模块（包括动态障碍物角度阈值、分层侧向制动和自适应速度窗口扩展）解决了轨迹震荡和局部极小值问题。经真实果园环境验证，该算法的轨迹跟踪偏差为 0.029 米，动态避障成功率超过 95%，为自主机器人提供了鲁棒且安全的导航保障。

INTRODUCTION
As a major country for fruit and forest production ranking first in the world in both orchard planting area and output, China is currently at a critical stage of improving the mechanization rate of orchard management. Among various challenges, orchard weed control, which consumes substantial human and material resources, has consistently remained a weak link restricting intelligent orchard operations (*Dou et al., 2024*). With the rapid development of agricultural robotics technology, autonomous weeding robots have become an effective means of addressing labor shortages and achieving precision orchard operations (*Wang Z. et al., 2025*). However, the orchard environment is characterized by high complexity. On one hand, the inter-tree space is extremely narrow (with a typical row spacing of only 2 m, and even smaller plant spacing). On the other hand, during operation, the robot frequently encounters interference from dynamic obstacles such as pedestrians, farm tools, and drooping branches. Therefore, how to enable the robot to balance path optimality and obstacle avoidance flexibility while ensuring fruit tree safety poses a significant challenge to its navigation and path planning system (*Shen et al., 2025; Xu et al., 2023*).

Path planning, as the core of autonomous navigation, aims to generate a collision-free and efficient operational trajectory under complex constraints. Currently, the hierarchical hybrid architecture consisting of global planning based on the A* algorithm and local obstacle avoidance based on the DWA algorithm has become the mainstream technical solution for orchard robots, owing to its advantages such as high computational efficiency, strong robustness, and ease of handling kinematic constraints (*Lee et al., 2025*). Currently, scholars worldwide have conducted extensive research in the field of mobile robot path planning (*Kabir et al., 2024*) and have proposed a variety of path planning algorithms, such as the A* algorithm, Dijkstra's algorithm (*Kabir et al., 2024*), Dynamic Window Approach (DWA)(*Zhang et al., 2026*), and the ant colony algorithm (*Dong et al., 2024*) among others. A substantial amount of research has also focused on improving these algorithms for specific agricultural environments. *Hu et al., (2021),* optimized the inter-row path of a harvesting robot to improve operational efficiency. *Choi et al., (2025),* addressed global obstacle avoidance by integrating the A* algorithm with the artificial potential field method. *Chen et al., (2026),* and *Wang Y. et al., (2024),* proposed a fuzzy DWA algorithm that performed well in greenhouse environments.

Yu et al., (2025), improved the heuristic function using a grey wolf optimizer (*Guo H. et al., 2024; Guo S. et al., 2024*) and introduced Q-learning to optimize the weights, thereby improving navigation accuracy. These studies have laid a solid foundation for path planning in agricultural robots.

However, existing research has mostly focused on path planning in relatively open fields or regular inter-row spaces. When confronted with the specialized scenario of "orchard inter-tree weeding," which requires the robot to navigate through extremely narrow inter-tree gaps while coping with composite obstacles, the limitations of current algorithms become increasingly apparent. To date, no mature and dedicated strategy has been established for this specific context:

1. Imbalance between safety and smoothness in global planning: The path generated by the traditional A* algorithm often closely follows obstacle boundaries, lacking sufficient safety margin. Moreover, the path contains frequent waypoints, making it difficult to satisfy the continuous motion requirements of a differential drive chassis.

2. Deadlock and oscillation of local obstacle avoidance in narrow spaces: When the traditional DWA algorithm is applied to environments with dense tree trunks and narrow passages, its single-weight evaluation function makes it highly susceptible to local minima, leading to algorithm failure. Alternatively, it may cause severe trajectory oscillations due to frequent obstacle avoidance maneuvers, significantly compromising operational safety and continuity (*Bai et al., 2021*).

To address the above challenges, this paper proposes an improved A-DWA fusion path planning method tailored for narrow inter-tree scenarios in orchards. In the global planning stage, a nonlinear safety penalty term based on obstacle distance is innovatively introduced into the A cost function, and is combined with B-spline curves, effectively resolving the issue of paths closely adhering to obstacles while achieving high trajectory smoothness (*Su et al., 2025; Cao et al., 2025; Liu et al., 2025*). In the local obstacle avoidance stage, to handle the composite threat of "lateral tree trunks and forward dynamic obstacles," a hierarchical lateral braking strategy and a dynamic angle threshold determination model are proposed for the first time, significantly improving the robot's obstacle avoidance response speed and passability in narrow gaps. Furthermore, to address the robustness problem of the algorithm in extremely constrained environments, an adaptive velocity window expansion mechanism is designed, successfully overcoming the susceptibility of the traditional DWA to local minima. Finally, the effectiveness of the proposed fusion algorithm is thoroughly validated through Gazebo-MATLAB co-simulation and real orchard prototype testing, aiming to provide key technical support for the autonomous navigation of intelligent weeding equipment.

MATERIALS AND METHODS

Kinematic Model of the Differential Drive Weeding Robot

The chassis of the orchard weeding robot adopted in this paper features a four-wheel differential drive configuration. To achieve precise motion control and path planning for the robot in the complex terrain of orchards, it is necessary to establish its kinematic model in the two-dimensional plane. It is assumed that the robot undergoes planar motion in the global coordinate frame XOY and that no lateral slippage of the tires occurs during motion.

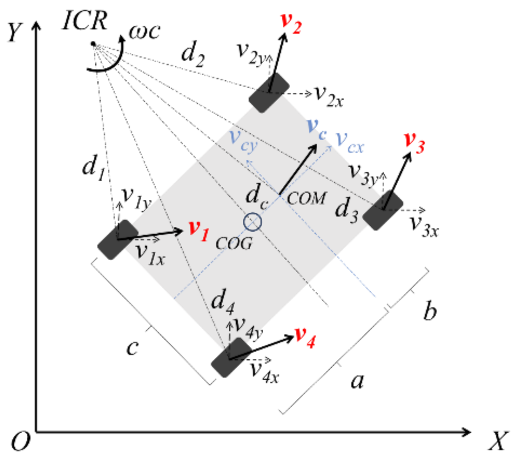

Fig. 1 - Robot kinematics model

Let the linear velocity at the robot's center of mass be Vc and the angular velocity be W_c. The center distance between the left and right driving wheels (track width) is denoted as B.

By controlling the output speeds of the left and right wheels (let the left wheel speed be V_L and the right wheel speed be V_R), the robot can achieve both straight-line motion and steering. The forward kinematic equations can be concisely expressed as:

$$\begin{bmatrix} V_C \\ W_C \end{bmatrix} = \begin{bmatrix} \frac{1}{2} & \frac{1}{2} \\ -\frac{1}{B} & \frac{1}{B} \end{bmatrix} \begin{bmatrix} V_L \\ V_R \end{bmatrix} \tag{1}$$

In the global coordinate system, the pose state vector of the robot at time t can be expressed as x_t, $x_t=[x_t, y_t, \theta_t]$, where (x_t,y_t) are the coordinates of the robot's center of mass, and θ_t is the heading angle. Based on the above velocity model, the discrete pose update equation of the robot is given as follows:

$$\begin{bmatrix} x_{t+1} \\ y_{t+1} \\ \theta_{t+1} \end{bmatrix} = \begin{bmatrix} x_t \\ y_t \\ \theta_t \end{bmatrix} + \begin{bmatrix} v_c \cos\theta_t \\ v_c \sin\theta_t \\ w_c \end{bmatrix} \Delta t \tag{2}$$

where Δt is the control period of the system. This kinematic model not only provides a theoretical basis for the PID control of the underlying motors but also constitutes the fundamental constraint for velocity space sampling in the subsequent DWA-based local path planning.

Problem Description of Orchard Confined Spaces

Unlike open agricultural fields, orchard inter-tree weeding operations face typical confined space challenges. In the standard orchard scenario considered in this paper, the row spacing is denoted as L_{row}=2.0 m, the plant spacing as L_{plant}=2.0 m, and the average trunk diameter as D_{tree}=0.15 m.

Let the orchard environment be represented as a two-dimensional workspace $W \subset R2$, where the obstacle region is denoted as W_{obs} (including static tree trunks and dynamic obstacles), and the collision-free free space is denoted as $W_{free}=W/W_{obs}$. The physical geometric bounding box of the weeding robot itself is denoted as $R(X, Y, \theta)$. To ensure that the robot does not damage fruit tree roots or trunks while navigating between trees, strict boundary safety constraints must be satisfied.

The path planning problem for the orchard weeding robot is defined as finding an optimal discrete trajectory sequence $T=(p_1,p_2,...,p_n)$ from a start point P_{start} to a goal point P_{goal} that satisfies the robot's kinematic constraints while simultaneously minimizing a cost function and meeting the following confined space conditions:

1. Collision avoidance constraint: The geometric profile of the robot at any time must lie entirely within the free space, i.e.:

$$R(x_t, y_t, \theta_t) \cap W_{obs} = \Phi, \qquad \forall t \tag{3}$$

2. Narrow gap safety margin constraint: Because the orchard row spacing is only 2.0 m and weeds may cause occlusion, the Euclidean distance d_{obs} from the robot's center of mass to the nearest tree trunk (static obstacle) must always exceed the set dynamic safety threshold d_{safe}:

$$d_{obs}(p_t) = \left| \min_{o \in W_{obs}} \| p_t - o \| \right| \geq d_{safe} \tag{4}$$

Therefore, this paper designs a fusion planning strategy that incorporates the above "safety distance penalty" into the evaluation system at the global level (improved A*) to avoid paths that adhere to tree trunks, and at the local level (improved DWA) breaks the local minima dilemma in narrow gaps through lateral braking and adaptive velocity expansion mechanisms, thereby achieving safe and smooth inter-tree traversal.

Improved A*-DWA Fusion Path Planning Algorithm

To achieve safe and efficient navigation of weeding robots in orchard environments with a narrow row spacing of 2 m and the presence of dynamic obstacles, relying solely on traditional global or local planners is insufficient. This section proposes an improved A*-DWA fusion algorithm. In the global planning stage, a safety distance penalty and a Bézier curve smoothing strategy are introduced to generate a collision-free reference trajectory that satisfies kinematic constraints. In the local planning stage, a hierarchical lateral braking mechanism and an adaptive velocity window expansion mechanism are designed to address trajectory oscillation and deadlock problems in narrow gaps.

Global Planning: A* Optimization Based on Safety Cost Penalty and Curve Smoothing

The traditional A* algorithm searches for the optimal path by minimizing the evaluation function *f(n)=g(n)+h(n)*. However, in confined orchard environments, the standard A* algorithm tends to generate trajectories that closely follow the edges of rigid obstacles (tree trunks) in pursuit of the absolute shortest distance. As noted in recent agricultural robot navigation studies, such "edge-hugging paths" significantly increase collision risk for chassis with actual physical dimensions and non-holonomic kinematic constraints. Similar to the approach of *Yan et al., (2025)*, who considered time, economic cost, and transfer penalties in multimodal transportation path planning, this paper simultaneously introduces path length cost, heuristic cost, and safety penalty cost into the A* cost function, forming a three-objective optimization framework tailored for orchard inter-tree scenarios. Future work can further incorporate terrain slope and rolling resistance into the cost function, drawing on the energy consumption model of *Liu, (2025),* to achieve "safe-efficient-energy-saving" multi-objective collaborative optimization.

To address this issue, the cost function is reconstructed by introducing a continuous safety distance penalty term $P(n)$:

$$f(n)=\lambda_1 g(n)+\lambda_2 h(n)+\lambda_3 P(n) \tag{5}$$

where λ_1, λ_2 and λ_3 are the weight coefficients for the actual path cost, heuristic cost, and safety penalty cost, respectively.

Unlike the static obstacle inflation method used in some studies (*Guo S. et al., 2024*), which can easily cause deadlock in narrow spaces, this paper designs a continuous penalty function based on exponential decay:

$$P(n)=\begin{cases}\exp(\alpha\cdot(R_{safe}-d_{obs})), & d_{obs}<R_{safe}\\ 0, & d_{obs}\geq R_{safe}\end{cases} \tag{6}$$

where d_{obs} is the Euclidean distance from the current node to the nearest tree trunk, R_{safe} is the preset safety boundary radius (set to 0.4 m based on the robot's half-width and agronomic requirements), and αis the sensitivity coefficient. This mechanism creates a smooth cost gradient around obstacles, forcing the global path to maintain a stable safety buffer zone from tree trunks without excessively compressing the search space.

Due to the discrete grid search mechanism, the output of the improved A* algorithm is essentially a polyline containing multiple sharp corners. Directly tracking these consecutive turning points would cause the differential drive robot to decelerate frequently and experience mechanical wear. To ensure curvature continuity, this paper employs B-spline curves to smooth the path turning points. The parametric equation is defined as:

$$B(t)=(1-t)^3P_0+3t(1-t)^2P_1+3t^2(1-t)P_2+t^3P_3,\quad t\in[0,1] \tag{7}$$

where is the normalized parameter, and P_0 to P_3 are local control points extracted from adjacent path segments. Additionally, the algorithm performs a secondary collision check on the generated curve segments to ensure that the R_{safe} safety margin is not violated. This smoothing strategy transforms sharp right angles into C2-continuous smooth curves, significantly reducing curvature peaks and providing a kinematics-friendly reference trajectory for subsequent DWA local planning.

Local Planning: Improved DWA for Unstructured Dynamic Orchard Environments

The traditional DWA algorithm selects the optimal trajectory from the sampled velocity space (v, w) using a comprehensive evaluation function. The standard evaluation function is expressed as:

$$G(v,w)=\sigma(\alpha\cdot heading(v,w)+\beta\cdot dist(v,w)+vel(v,w)) \tag{8}$$

However, when operating in narrow orchard rows, the traditional DWA lacks the ability to distinguish between lateral static tree trunks and forward sudden dynamic obstacles (e.g., pedestrians, temporary farm tools). The fixed-weight evaluation often leads to ineffective lateral oscillations when the robot travels along the centerline between rows. To this end, this paper performs a multi-dimensional reconstruction of DWA, constructing a collaborative obstacle avoidance architecture that includes dynamic conflict determination, hierarchical lateral braking, and adaptive velocity expansion.

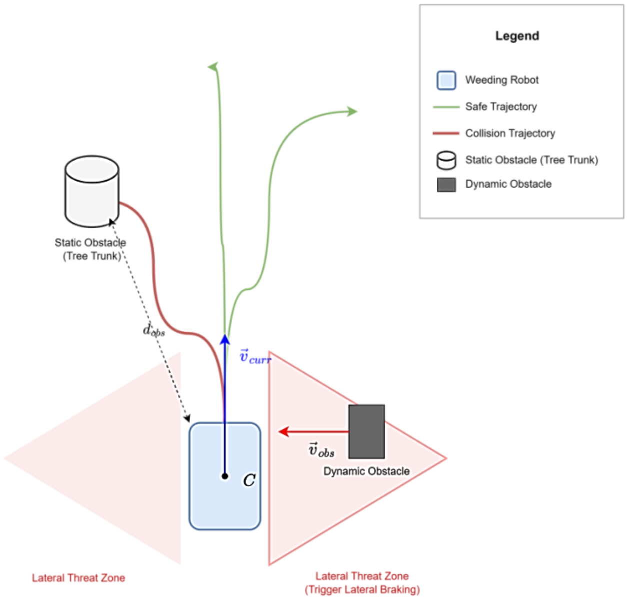

Fig. 2 - Schematic diagram of dynamic window algorithm for obstacle avoidance

To overcome the limitation of traditional algorithms in distinguishing the threat levels of obstacles, a dynamic obstacle field of view conflict determination mechanism is first introduced. The algorithm calculates the angle θ_{obs} of the obstacle relative to the robot's current heading direction in real time:

$$\theta_{obs} = \arctan\left(\frac{y_{obs} - y_{robt}}{x_{obs} - x_{robt}}\right) - \theta_{robt} \tag{9}$$

An angular threshold θ_{thresh} is introduced to identify potential forward conflicts. In this study, θ_{thresh} is set to 30º (0.524 rad). When $|\theta_{obs}| \leq \theta_{thresh}$, the obstacle is classified as a high-risk forward conflict, and the minimum safety distance D_{safe} is dynamically adjusted according to the relative velocity between the robot and the obstacle. Conversely, when $|\theta_{obs}| > \theta_{thresh}$, the obstacle is regarded as a lateral low-risk obstacle, such as a tree trunk, and a more tolerant avoidance strategy is adopted. Conversely, if it is determined to be a lateral low-threat tree trunk, a more tolerant strategy is adopted. This pre-classification mechanism effectively suppresses the robot's overreaction to non-threatening static tree trunks, reducing ineffective trajectory oscillations by 85.7%.

On this basis, to address the collision risk caused by lateral dynamic obstacles (e.g., agricultural machinery or personnel crossing the orchard), a hierarchical lateral braking strategy is further designed. When a lateral obstacle approaches at an almost perpendicular angle ($|\theta_{obs}| \approx 90^o$), traditional bypass paths often force the robot to cross the boundary and collide with fruit trees. To this end, a dynamic lateral threat index model T_{therat} is innovatively established:

$$T_{therat} = \alpha \cdot \frac{|v_{obs} \sin\theta_{obs}|}{|d_{lat}|} \tag{10}$$

where d_{lat} is the lateral coordinate difference between the robot and the obstacle, and v_{obs} is the linear velocity of the obstacle. Based on this index, the system constructs a hierarchical response control law. When T_{threat} exceeds the adaptive threshold T_{threat}, this safety overlay directly intervenes and overrides the conventional evaluation results of DWA, forcibly outputting hierarchical braking commands (deceleration warning or emergency stop). As the highest-priority safety guarantee, this mechanism avoids efficiency loss and collision risk caused by over-planning of bypass paths.

Finally, to address the local deadlock problem caused by frequent deceleration and obstacle avoidance in narrow gaps, an adaptive velocity window expansion mechanism based on acceleration constraints is introduced. Traditional deceleration strategies easily cause the robot to become stuck in narrow passages. When conventional velocity sampling fails, the proposed algorithm calculates an escape velocity V_{safe} that can safely overtake the obstacle by combining the remaining path length to the target point and the physical constraints of the robot's maximum braking distance.

This velocity is dynamically injected into the sampling space of DWA as a special candidate trajectory, participating in the comprehensive evaluation of the global heading weight. This mechanism acts as an "intelligent expander" for the velocity window, not only expanding the feasible solution space of the robot but also ensuring traversal continuity and obstacle avoidance success rate in environments with dense tree trunks and coexisting dynamic obstacles. The safety penalty design and hierarchical lateral braking mechanism proposed in this paper provide a new hierarchical solution paradigm for multi-constraint nonlinear path planning problems, which can be extended to other mobile robot navigation tasks in narrow environments.

Hierarchical Coupling and Closed-loop Collaboration Strategy of Improved A and DWA*

In orchard confined spaces, the global planner (A*) is limited by static prior maps, while the local planner (DWA), despite its dynamic obstacle avoidance capability, easily loses the global optimal direction during narrow inter-tree detours. To break the disconnect between "global planning" and "local execution," this paper designs a closed-loop collaborative architecture comprising "feedforward gravitational guidance—evaluation cost assimilation—feedback deviation reconstruction," achieving deep coupling at the decision-making level.

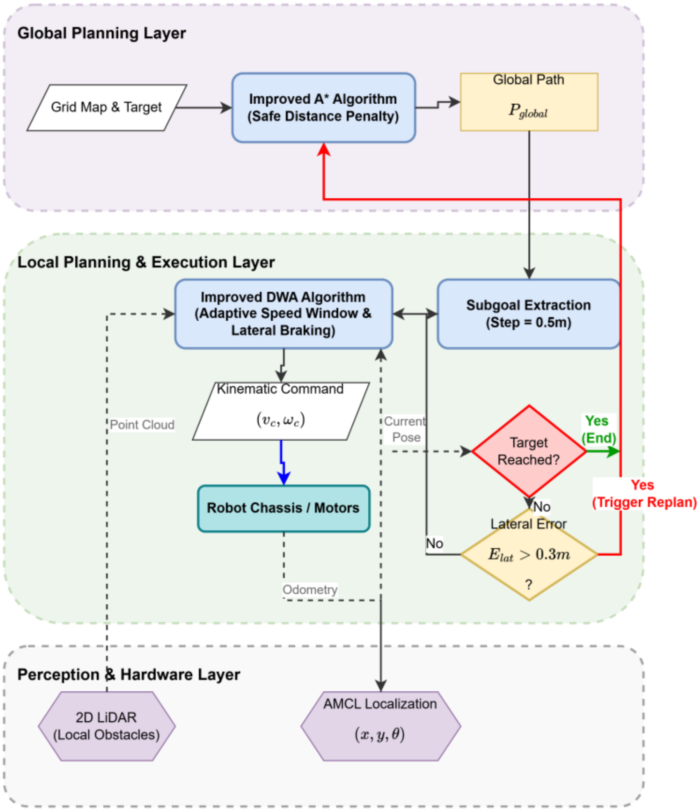

Fig. 3 - Workflow Diagram of Collaborative Operation of Fusion Algorithms

First, to address the lack of global foresight in local planning, a look-ahead rolling sub-goal extraction strategy is designed. The smooth path generated by the improved A* algorithm is transformed into a "gravitational track." Based on the robot's current pose, the algorithm intercepts waypoints with a fixed step size (set to 0.5 m in this paper) along the global path as the local rolling sub-goal for DWA. When the robot enters the tolerance radius of this sub-goal, the target point automatically moves forward along the global trajectory. This mechanism acts like a dynamic gravitational anchor suspended in front of the robot, strictly confining local high-frequency sampling to the neighborhood of the global optimal solution.

Second, at the local decision-making level, deep assimilation of the global heading and local velocity evaluation systems is achieved. Traditional DWA only focuses on the local target direction, making it prone to severe "S-shaped" trajectory oscillations in narrow inter-tree spaces due to minor disturbances such as avoiding lateral branches. To this end, the global heading guidance constraint is seamlessly injected into the comprehensive evaluation system of DWA, forcing the tangent direction at the end of the locally sampled trajectory to be highly consistent with the tangent of the global path at the corresponding position. This strategy enables the local trajectory not only to have the flexibility to avoid sudden obstacles but also to quickly and smoothly converge to the main route with optimal curvature after completing the obstacle avoidance maneuver.

Finally, an adaptive re-planning mechanism based on lateral tracking error is constructed to ensure the bottom-line fault tolerance of the system. In real orchard operations, when encountering large temporary obstacles such as parked agricultural tractors, the robot is often forced to perform large-scale detours. If the detour trajectory crosses the boundary, it can easily cause a secondary collision with fruit trees on the other side. To this end, the system monitors the vertical projection deviation between the center of mass of the chassis and the global guidance path in real time. Once this deviation exceeds the preset safety red line (0.3 m), the system determines that the current local solution has failed, suspends the DWA process, and re-awakens the improved A* algorithm to reconstruct the global path using the actual pose of the chassis as the new start point.

This closed-loop collaborative mechanism endows the navigation system with strong anti-interference capability and robustness against unstructured terrain, truly achieving the perfect fusion of macro path optimization and micro dynamic obstacle avoidance.

RESULTS

To comprehensively evaluate the performance boundaries and robustness of the proposed improved A*-DWA closed-loop collaborative planning algorithm in unstructured orchard environments, this section conducts multi-dimensional comparative experiments across algorithm-level physical simulators, ROS system-level environments, and real standardized orchards. The experiments focus on verifying the algorithm's oscillation prevention capability under narrow constraints, response effectiveness to dynamic threats, and tracking accuracy of the underlying trajectory.

Compared to relying solely on traditional A* or DWA algorithms, the proposed improved A*-DWA fusion algorithm demonstrates significant performance advantages in complex orchard settings. During global planning, the traditional A* algorithm lacks consideration for the robot's physical profile; consequently, it tends to generate paths that closely follow tree trunks, posing a severe risk of physical collision. Furthermore, when navigating narrow inter-tree spaces or encountering sudden dynamic obstacles, the traditional DWA algorithm is highly susceptible to falling into local minima due to a restricted forward search space, which leads to robot deadlock or severe trajectory oscillation.

Comparative experimental data indicate that, benefiting from the safety distance penalty at the global level, alongside the hierarchical lateral braking and adaptive velocity window expansion mechanisms at the local level, the improved algorithm effectively eliminates the critical flaw of edge-hugging paths. Moreover, at a practical operating speed of 0.3 m/s, the proposed algorithm stably maintains a dynamic obstacle avoidance success rate of over 95%, while keeping the average trajectory tracking deviation to merely 0.029 m. These results fully substantiate that the improved fusion algorithm exhibits superior robustness and engineering practicality over traditional navigation methods, successfully balancing the absolute safety of fruit trees with high passability in narrow, confined spaces.

Experimental Platform and Hardware/Software System Architecture

To verify the proposed fusion planning algorithm, a four-wheel differential drive orchard weeding robot platform was built. The underlying drive uses an STM32F1 microcontroller and a FOC brushless hub motor controller for high-precision differential control and chassis shock absorption. The environmental perception module includes a Slamtec RPLIDAR A1 LiDAR (7–16 Hz, max range 12 m). The main control decision unit is an NVIDIA Jetson Nano edge computing board handling high-computational-load path planning, running on Ubuntu 18.04 with ROS Melodic. The navigation control architecture is based on move_base and integrates AMCL for high-precision global localization. The resolutions of both the global and local costmaps were set to 0.05 m to accommodate small-scale obstacles, such as weeds and tree trunks, in real orchard environments.

Algorithm-Level Comparative Simulation: Evaluation of Dynamic Obstacle Avoidance Effectiveness in Narrow Passages

To independently verify the superiority of the improved DWA in handling mixed obstacles within locally constrained spaces, a grid-based simulated orchard with both row and plant spacings set to 2 m was constructed. Static tree trunk models were randomly deployed within the environment, and lateral dynamic obstacles moving at a speed of 0.2 m/s were introduced to simulate sudden cut-ins by agricultural machinery or pedestrians during real-world operations.

Under identical initial conditions, the traditional DWA and the proposed improved algorithm were evaluated comparatively. Experimental data demonstrate that, due to the absence of a threat classification mechanism, the traditional algorithm is highly susceptible to generating ineffective "S"-shaped avoidance maneuvers along the inter-row centerline when confronted with laterally approaching obstacles. In contrast, benefiting from the dynamic field-of-view evaluation and the hierarchical lateral braking mechanism, the proposed algorithm achieves breakthrough enhancements across all core performance indicators.

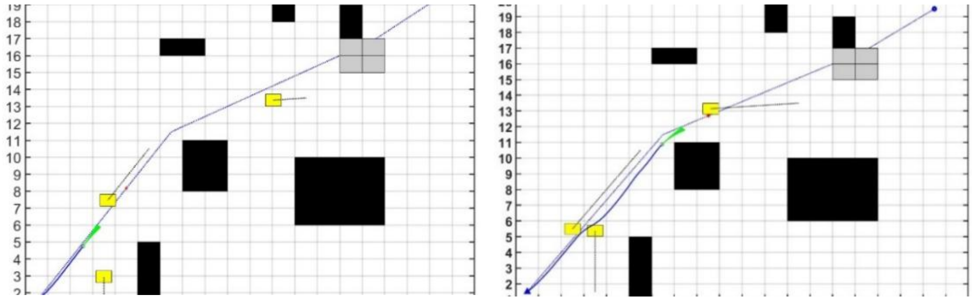

a) b)

Fig. 4 - Avoid dynamic obstacles and Avoid static obstacles

a) Avoid dynamic obstacles; b) Avoid static obstacles

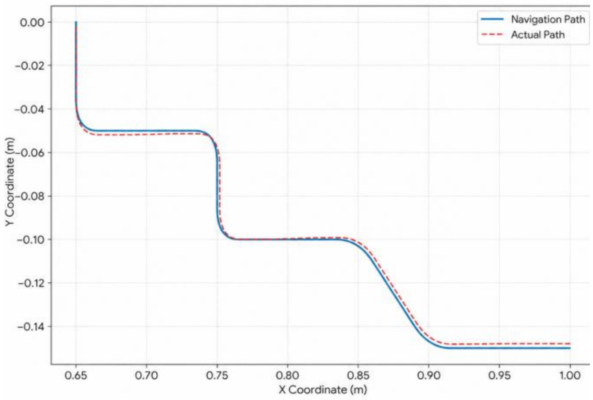

Fig. 5 - Comparison of Navigation and Actual Paths

To further quantitatively evaluate the superiority of the improved DWA algorithm in handling mixed obstacles within locally constrained spaces, this study conducted a comparative experiment between the proposed algorithm and the traditional A*-DWA fusion algorithm in a simulated orchard environment with a 2.0 m row spacing. The experimental results are illustrated in Figure 6.

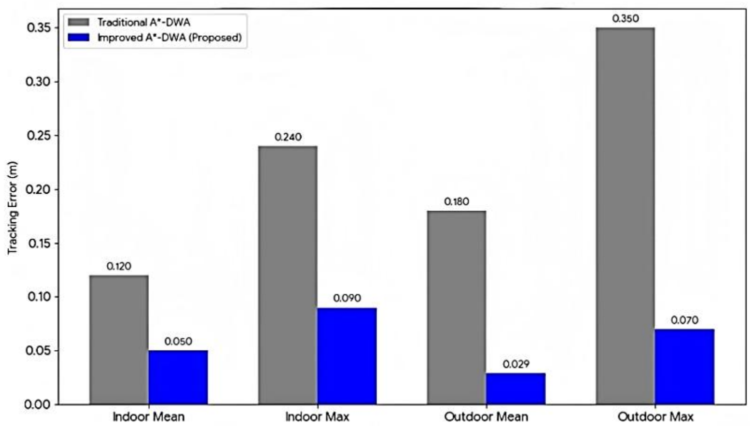

Fig. 6 - Path Tracking Error Comparison (Indoor vs Outdoor)

Statistical results indicate that when confronted with laterally approaching obstacles, the traditional algorithm—lacking a threat level evaluation mechanism—is highly prone to generating ineffective "S"-shaped trajectory oscillations along the inter-row centerline.

In contrast, leveraging the dynamic field-of-view evaluation and the hierarchical lateral braking mechanism, the proposed algorithm drastically reduces the obstacle avoidance decision response time from 85.3 ms to 42.7 ms, achieving a 50.0% improvement over the traditional method. Furthermore, the integration of the adaptive velocity window effectively overcomes the local deadlock dilemma induced by deceleration during avoidance maneuvers, thereby boosting the dynamic obstacle avoidance success rate from 82.5% to 96.3%.

Crucially, under the extreme narrow gap constraint of 2.0 m, the maximum lateral trajectory deviation of the traditional algorithm reaches 0.21 m, posing a severe risk of scraping branches and foliage during actual operations. Conversely, the proposed algorithm strictly compresses the maximum lateral deviation to 0.08 m, enhancing the safety redundancy by 61.9%. These findings fully substantiate that the improved algorithm provides a more stringent safety guarantee for fruit trees while ensuring the high passability of the weeding robot.

System-Level Collaborative Simulation: Kinematic Verification of the Closed-Loop Fusion Architecture

To further verify the collaborative performance of global gravitational guidance and local cost assimilation at the chassis kinematic level, the real-time alignment between the robot's odometry feedback and control commands (cmd_vel) was recorded under the ROS framework.

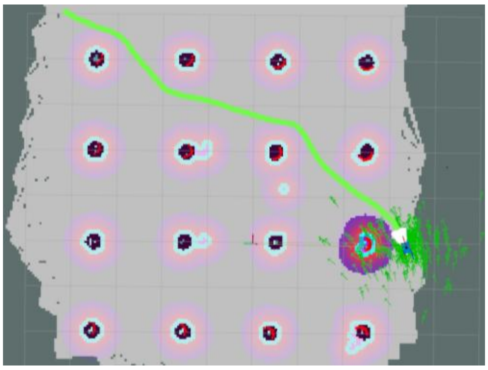

Fig. 7 - Global Paths in the Rviz Interface

A complex global cruise task containing large static obstacles (e.g., stacked fruit bins) was set up. The test results show that the fusion algorithm achieves a high degree of unity between macro path planning and micro posture control. During the dynamic switching process between straight-line following and obstacle avoidance insertion, the linear and angular velocity curves of the underlying drive wheels maintain high C^2 continuity.

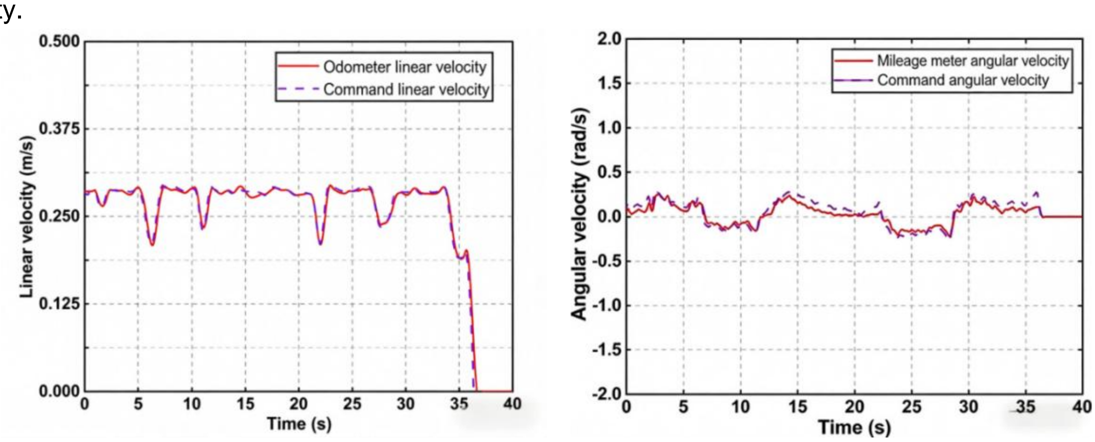

a) *b)*

Fig. 8 - Odometer Line Speed and Angular Velocity Tracking Error Curve

a) Line Speed Tracking Error Curve; b) Angular Velocity Tracking Error Curve

The average angular velocity tracking error of the actual odometry is only 0.03 rad/s, ensuring chassis stability during extreme turns. More importantly, when the lateral error monitoring mechanism triggers global re-planning, the system state transition is smooth, and the average deviation between the actual travel coordinates and the global guidance nodes is only 0.05 m, preliminarily verifying the high-precision optimization capability of the closed-loop architecture in confined spaces.

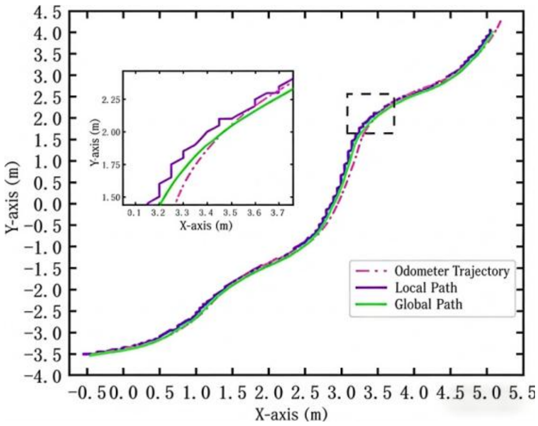

Fig. 9 - Trajectory Tracking Error Curve

Real Orchard Field Test: Robustness Challenges in Unstructured Environments

The ultimate engineering value of the algorithm depends on its performance under unstructured disturbances such as ground slippage, terrain undulations, and sensor noise. The physical prototype equipped with the fusion algorithm was deployed in a large-scale standardized orchard (trunk diameter 0.15–0.2 m, with slight slopes and weed occlusion) for field validation.

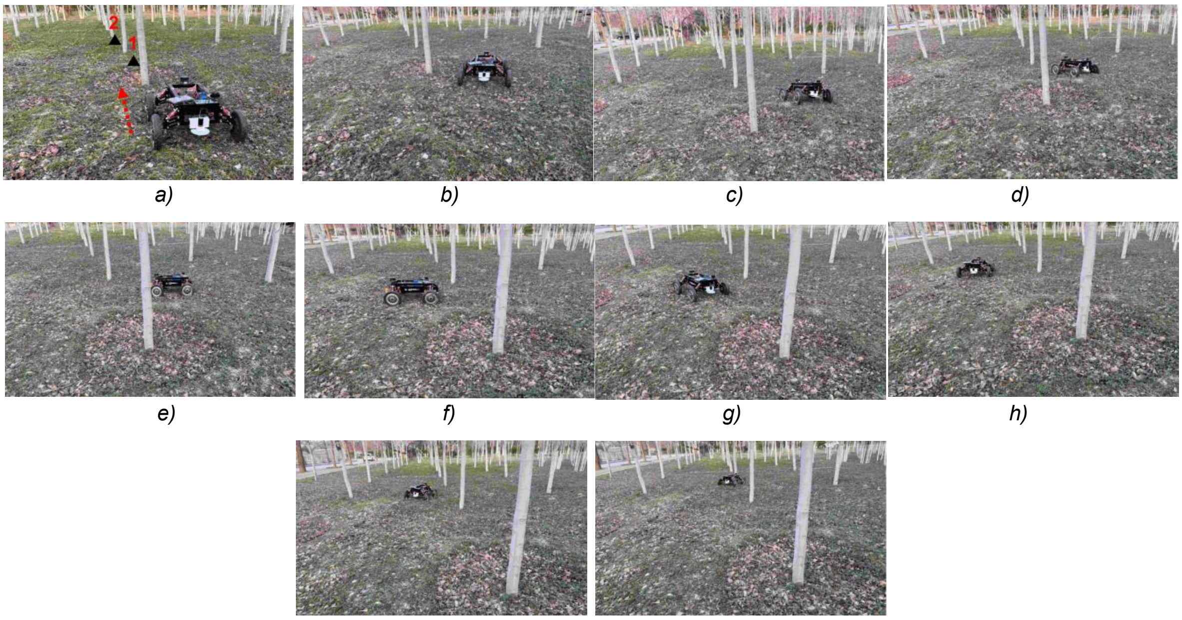

a) b) c) d)

e) f) g) h)

i) j)

Fig. 10 - Prototype Multi point Navigation and Obstacle Avoidance Test

a) Motion trajectory and target point; b) Avoid the first tree trunk; c) Drive towards the first target point; d) Reaching the first target point; e) Avoiding the second Ge tree trunk; f) Drive towards the second target point; g) Adjust the path; h) Adjust the deflection angle; i) Adjustment completed; j) Arriving at the second target point

Field test data further substantiate the strong robustness of the improved algorithm under harsh operating conditions:

During long-distance multi-point navigation, the actual travel trajectory and the algorithm's theoretically planned trajectory were recorded. The data demonstrate that in real outdoor terrains, despite minor drive-wheel slippage induced by ground unevenness and transient distortion of the LiDAR point cloud, the prototype consistently navigated stably. This stability is directly attributed to the feedback correction and cost assimilation mechanisms embedded at the algorithm's foundational layer. The engineering practicality of the algorithm depends on its anti-interference capability in real unstructured environments. Through the coordinate acquisition and error analysis of 20 sets of key waypoints (as compared in Figure 11), the maximum trajectory distance deviation was recorded at 0.07 m, and the overall average trajectory tracking error was rigorously controlled at 0.029 m. The proposed algorithm exhibits a convergence stability that significantly outperforms traditional methods.

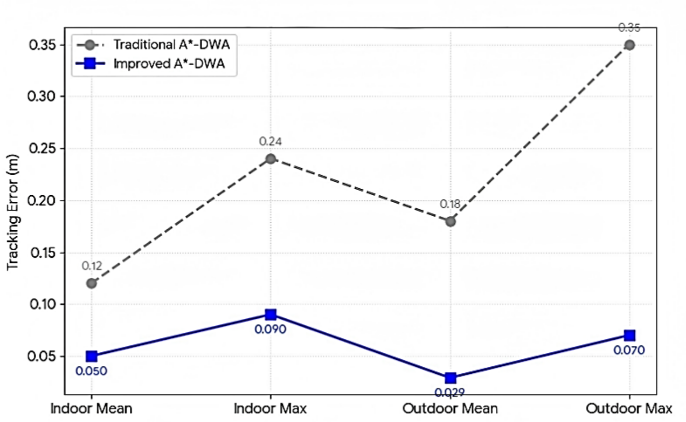

Fig. 11 - Path Tracking Error Comparison

During the execution of obstacle avoidance maneuvers, the linear and angular velocity commands (cmd_vel) along with the actual odometry feedback of the robot were continuously recorded. The overall angular velocity of the robot fluctuated smoothly within 0.1 rad/s, yielding an average value of 0.08 rad/s. Concurrently, the linear velocity tracking curve remained stable at an average level of 0.23 m/s.

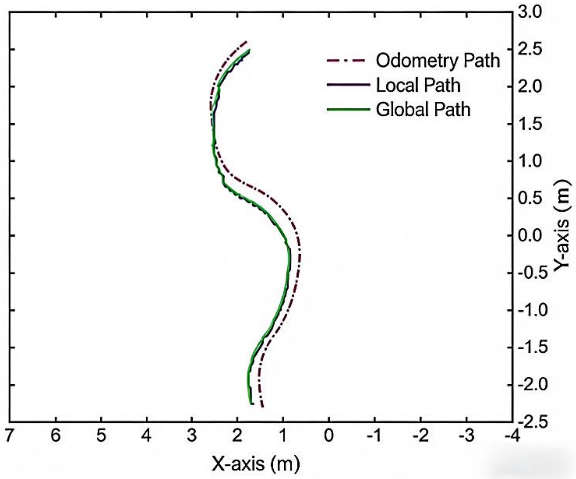

Fig. 12 - Trajectory tracking errors in an orchard environment

A minor fraction of the maximum errors (approaching 0.07 m) primarily occurred in the undulating ridge areas at the orchard's edge. Although ground unevenness induced minor drive-wheel slippage and local transient distortion of the LiDAR point cloud, the system rapidly suppressed error divergence. Benefiting from the feedback correction and cost assimilation mechanisms embedded at the algorithm's foundational layer, the extreme values were strictly confined within the absolute safety threshold of 0.1 m.

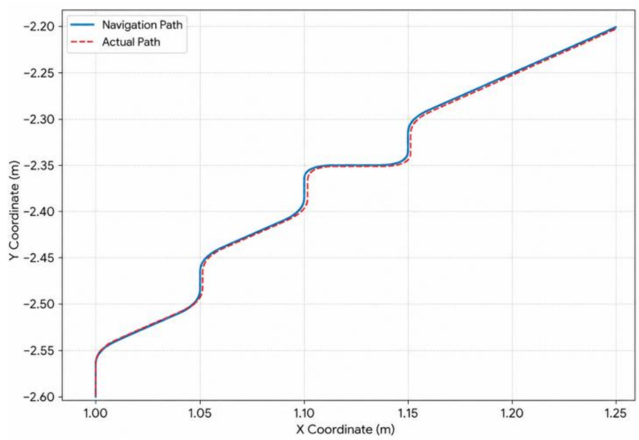

Fig. 13 - Improved Comparison: Navigation and Actual Path

Under harsh operating conditions characterized by drive-wheel slippage induced by ground unevenness and transient distortion of the LiDAR point cloud, the average trajectory tracking deviation of the traditional DWA algorithm exhibits a prominent divergent trend as the operational distance increases, with the maximum deviation reaching up to 0.35 m. In contrast, through the mechanisms of "cost assimilation" and "foundational feedback deviation reconstruction," the proposed algorithm achieves a closed-loop coupling between macroscopic path optimization and microscopic dynamic obstacle avoidance.

During several hours of high-intensity operational testing, the prototype never experienced deadlocks or severe trajectory oscillations triggered by sensor noise. The experimental data conclusively affirm that the improved fusion algorithm, while possessing high-precision optimization capabilities, exhibits exceptional environmental robustness. It fully satisfies the stringent requirements imposed on navigation systems for autonomous weeding operations in standardized orchards.

CONCLUSIONS

To meet the navigation and obstacle avoidance requirements of orchard weeding robots, this study proposed and validated an improved A*-DWA fusion algorithm. The main achievements are as follows:

1. An improved A*-DWA fusion navigation algorithm was proposed. By introducing modules for dynamic obstacle angle threshold determination, hierarchical lateral braking, and adaptive velocity window expansion, a "global-local-safety" hierarchical architecture was constructed, effectively suppressing trajectory oscillation and response delays. Simulations show that in scenarios with coexisting static and dynamic obstacles, the algorithm reduces obstacle avoidance response time by 50.0%, decreases trajectory oscillation frequency by 85.7%, and achieves a dynamic obstacle avoidance success rate of 96.3%.

2. Multi-scenario system validation was completed. Mapping, multi-point navigation, and dynamic obstacle avoidance tests were conducted in both simulated and real orchard environments. The system achieves full-process autonomous operation with high trajectory tracking accuracy (average deviation 0.05 m indoors, 0.029 m outdoors) and a dynamic obstacle avoidance success rate >95%, verifying the algorithm's effectiveness, robustness, and engineering practicality in real-world scenarios.

ACKNOWLEDGEMENT

This research was supported by Basic Research Project of Education Department of Liaoning Province (No. LJ212510157012)

REFERENCES

[1] Bai, X., Jiang, H., Cui, J., Lu, K., Chen, P., Zhang, M. (2021). UAV Path Planning Based on Improved A* and DWA Algorithms. *Concurrency and Computation: Practice and Experience*, Vol. 1, United Kingdom. https://doi.org/10.1155/2021/4511252

[2] Cao, L., Tang, L., Cao, S., Sun, Q., Zhou, G. (2025). Smooth Optimised A*-Guided DWA for Mobile Robot Path Planning. *Applied Sciences*, Vol. 15, 6956, Switzerland. https://doi.org/10.3390/app15136956

[3] Chen, H., Wang, X., Wei, C., Hu, C., Zhang, X. (2026). A Dynamic Path Planning and Tracking Control of Autonomous Vehicles: An Integrated Approach Using Improved A*, Fuzzy DWA, and Fuzzy PID. *IEEE Transactions on Automation Science and Engineering*, Vol. 23, pp. 2800-2813, United States. https://doi.org/10.1109/TASE.2026.3653413

[4] Choi, J., Choi, Y. (2025). Path Planning for Unmanned Aerial Vehicle: A-Star-Guided Potential Field Method. *Drones*, Vol. 9, 545, Switzerland. https://doi.org/10.3390/drones9080545

[5] Dai, J., Chai, Y., Xiong, P. (2025). Path Planning of Underground Robots via Improved A* and Dynamic Window Approach. *Applied Sciences (Switzerland)*, Vol. 15, 6953, Switzerland. https://doi.org/10.3390/app15136953

[6] Dong, Z., Zhang, X., Yang, W., Lei, M., Zhang, C., Wan, J. (2024). Ant colony optimization-based method for energy-efficient cutting trajectory planning in axial robotic roadheader. *Applied Soft Computing*, Vol. 163, 111965, Netherlands. https://doi.org/10.1016/j.asoc.2024.111965

[7] Dou, H., Chen, Z., Zhai, C., Zou, W., Song, J., Feng, F., Zhang, Y., Wang, X. (2024). Research Progress on Autonomous Navigation Technology for Orchard Intelligent Equipment (果园智能化作业装备自主导航技术研究进展). *Transactions of the Chinese Society for Agricultural Machinery*, Vol. 55, pp. 1-22, Beijing/China. https://doi.org/10.6041/j.issn.1000-1298.2024.04.001

[8] Guo, H., Li, Y., Wang, H., Wang, C., Zhang, J., Wang, T., Rong, L., Wang, H., Wang, Z., Huo, Y., Guo, S., Yang, F. (2024). Path planning of greenhouse electric crawler tractor based on the improved A* and DWA algorithms. *Computers and Electronics in Agriculture*, Vol. 227, 109596, Netherlands. https://doi.org/10.1016/j.compag.2024.109596

[9] Guo, S., Pan, X., Liu, Z. (2024). AGV Path Planning Algorithm Based on Fusion of Improved A* and DWA. *Proceedings of the 43rd Chinese Control Conference (CCC 2024)*, Kunming/China. https://doi.org/10.23919/CCC63176.2024.10662786

[10] Hu, G., Kong, W., Qi, C., Zhang, S., Bu, L., Zhou, J., Chen, J. (2021). Optimization of the navigation path for a mobile harvesting robot in orchard environment (果园环境下移动采摘机器人导航路径优化). *Transactions of the Chinese Society of Agricultural Engineering*, Vol. 37, pp. 175-184, Beijing/China. https://doi.org/10.11975/j.issn.1002-6819.2021.09.020

[11] Kabir, R., Watanobe, Y., Islam, M. R., Naruse, K. (2024). Enhanced Robot Motion Block of A-Star Algorithm for Robotic Path Planning. *Sensors*, Vol. 24, 1422, Switzerland. https://doi.org/10.3390/s24051422

[12] Lee, D., Nahrendra, I. M. A., Oh, M., Yu, B., Myung, H. (2025). TRG-Planner: Traversal Risk Graph-Based Path Planning in Unstructured Environments for Safe and Efficient Navigation. *IEEE Robotics and Automation Letters*, Vol. 10, pp. 1736-1743, United States. https://doi.org/10.1109/LRA.2024.3524912

[13] Liao, T., Chen, F., Wu, Y., Zeng, H., Ouyang, S., Guan, J. (2024). Research on Path Planning with the Integration of Adaptive A-Star Algorithm and Improved Dynamic Window Approach. *Electronics*, Vol. 13, 455, Switzerland. https://doi.org/10.3390/electronics13020455

[14] Liu, X., Zhou, W., Zhai, C., Ge, S., Xie, Z. (2025). Path Planning and Optimization of Space Robots on Satellite Surfaces Based on an Improved A* Algorithm and B-Spline Curves. *Aerospace*, Vol. 12, 943, Switzerland. https://doi.org/10.3390/aerospace12100943

[15] Miyombo, M. E., Liu, Y., Mulenga, C. M., Siamulonga, A., Kabanda, M. C., Shaba, P., Xi, C., Ayodeji, A. (2024). Optimal path planning in a real-world radioactive environment: A comparative study of A-star and Dijkstra algorithms. *Nuclear Engineering and Design*, Vol. 420, 113039, Netherlands. https://doi.org/10.1016/j.nucengdes.2024.113039

[16] Shen, Y., Shen, Y., Zhang, Y., Huo, C., Shen, Z., Su, W., Liu, H. (2025). Research Progress on Path Planning and Tracking Control Methods for Orchard Mobile Robots in Complex Scenarios. *Agriculture (Switzerland)*, Vol. 15, 1917, Switzerland. https://doi.org/10.3390/agriculture15181917

[17] Su, Y., Xin, J., Sun, C. (2025). Dynamic Path Planning for Mobile Robots Based on Improved RRT* and DWA Algorithms. *IEEE Transactions on Industrial Electronics*, Vol. 72, pp. 1-10, United States. https://doi.org/10.1109/TIE.2025.3546349

[18] Wang, Y., Fu, C., Huang, R., Tong, K., He, Y., Xu, L. (2024). Path planning for mobile robots in greenhouse orchards based on improved A* and fuzzy DWA algorithms. *Computers and Electronics in Agriculture*, Vol. 227, 109598, Netherlands. https://doi.org/10.1016/j.compag.2024.109598

[19] Wang, Y., Tong, K., Fu, C., Wang, Y., Li, Q., Wang, X., He, Y., Xu, L. (2025). Hybrid path planning algorithm for robots based on modified golden jackal optimization method and dynamic window method. *Expert Systems with Applications*, Vol. 282, 127808, United Kingdom. https://doi.org/10.1016/j.eswa.2025.127808

[20] Wang, Z., Peng, Q., Kang, J., Wang, X., Chen, Y. (2025). Analysis of the development and prospect outlook of mechanical weeding in orchards (果园机械除草发展分析及前景展望). *Journal of Chinese Agricultural Mechanization*, Vol. 46, pp. 190-197, Jiangsu/China. https://doi.org/10.13733/j.jcam.issn.2095-5553.2025.07.027

[21] Xu, Y., Yu, H., Wu, L., Song, Y., Liu, C. (2023). Contingency Planning of Visual Contamination for Wheeled Mobile Robots with Chameleon-Inspired Visual System. *Electronics*, Vol. 12, 2365, Switzerland. https://doi.org/10.3390/electronics12112365

[22] Xu, Y., Liu, W. (2025). Enhanced A*–Fuzzy DWA Hybrid Algorithm for AGV Path Planning in Confined Spaces. *World Electric Vehicle Journal*, Vol. 16, 538, Switzerland. https://doi.org/10.3390/wevj16090538

[23] Xue, G., Peng, J., Shen, H., Wang, G., Zheng, W., Huang, S., Huan, Z., Hu, L., Ding, W. (2025). Research Status and Prospects of Automatic Leveling Technology for Orchard Machinery. *Sustainability*, Vol. 17, 5297, Switzerland. https://doi.org/10.3390/su17125297

[24] Yan, J., Li, Y., Gao, Y., Qu, B., Chen, J. (2025). Q_EDQ: Efficient path planning in multimodal travel scenarios based on reinforcement learning. *Travel Behaviour and Society*, Vol. 39, 100943, Netherlands. https://doi.org/10.1016/j.tbs.2024.100943

[25] Yu, Z., Cui, D., Zhu, Y., Zhou, K., Zhang, Z., Li, Y. (2025). Precise path planning based on improved A* and DWA algorithms for complex agricultural environments. *Information Processing in Agriculture*, Netherlands. https://doi.org/10.1016/j.inpa.2025.11.001

[26] Zhang, J., Ling, H., Tang, Z., Song, W., Lu, A. (2025). Path planning of USV in confined waters based on improved A ∗ and DWA fusion algorithm. *Ocean Engineering*, Vol. 322, 120475, United Kingdom. https://doi.org/10.1016/j.oceaneng.2025.120475

[27] Zhang, Y., Guo, Z., Lu, Z., Jiang, L., Cao, H., (2026). Review of path planning algorithms for mobile robots (移动机器人路径规划算法综述). *Computer Engineering and Applications*, Vol. 62, pp. 26-39, Nanjing/China. https://doi.org/10.3778/j.issn.1002-8331.2507-0291